Clim. Past Discuss., 11, 1143–1175, 2015
www.clim-past-discuss.net/11/1143/2015/
doi:10.5194/cpd-11-1143-2015

Climate of the Past
Discussions
Open Access

Parallelisms between sea surface temperature changes in the western tropical Atlantic (Guiana basin) and high latitude climate signals over the last 140 000 years

O. Rama-Corredor[1], B. Martrat[1], J. O. Grimalt[1], G. E. López-Otalvaro[2], J. A. Flores[2], and F. Sierro[2]

[1]Department of Environmental Chemistry, IDAEA-CSIC, Barcelona, Catalonia, Spain
[2]Department of Geology, University of Salamanca, Plaza de la Merced s/n, 37008, Salamanca, Spain

Received: 31 January 2015 – Accepted: 11 February 2015 – Published: 2 April 2015

Correspondence to: J. O. Grimalt (joan.grimalt@idaea.csic.es)

Published by Copernicus Publications on behalf of the European Geosciences Union.

Abstract

Sea surface temperatures (SST) in the Guiana basin over the last 140 ka were obtained by measuring the C37 alkenone unsaturation index $U^{\prime k}_{37}$ in sediment core MD03-2616 (7° N, 53° W). The resulting dataset is unique for this period in the western tropical Atlantic region. SSTs range from 25.1 to 28.9 °C, i.e. glacial-to-interglacial amplitude of 3.8 °C, which is common in tropical areas.

During the last two interglacials (MIS1 and MIS5e) and warm long interstadials (MIS5d-a), the sediments studied trace rapid transmission of the climate variability from arctic-to-tropical latitudes and vice-versa. During these periods, MD03-2616 SSTs showed a remarkable parallelism with temperature changes observed in Greenland and SST records of North Atlantic cores.

The last deglaciation in Guiana is particularly revealing. MIS2 stands out as the coldest period of the interval analysed, with SSTs reaching as low as 25.1 °C. It contains reminders of northern latitude events such as the Bølling-Allerød warming and the Younger Dryas cooling which ensued. These oscillations were previously documented in the δ^{18}O of the Sajama tropical ice core and are present in Guiana with rates of ca. 6 °C ka^{-1} and changes of over 2 °C.

During the glacial interval, significant abrupt variability is observed; e.g. oscillations of 0.5–1.2 °C during MIS3, i.e. about 30 % of the maximum glacial–interglacial SST change. Nevertheless, in the MD03-2616 record it is hard to identify unambiguously either the Dansgaard–Oeschger type of oscillations described in northern latitudes or the SST drops associated with the Heinrich events characterising North Atlantic records. Although these specific events form the background of the climate variability observed, what truly shapes SSTs in Guiana is a long-term tropical response to precessional changes, which is modulated in the opposite way to polar variability. This lack of synchrony is consistent with other tropical records in locations to the north or south of Guiana and evidences an arctic-to-tropical decoupling when a substantial reduction in the Atlantic meridional overturning circulation (AMOC) takes place.

CPD
11, 1143–1175, 2015

1 Introduction

Abrupt climate changes have been recorded in a variety of environmental sensors and archives. Examples of these are: (i) isotopic composition of foraminifera (Bond et al., 1993; Lisiecki et al., 2005; McManus et al., 1994; Peterson et al., 2000; Shackleton et al., 2000) and sea surface temperatures (SST) derived from alkenones (Herbert and Schuffert, 2000; Martrat et al., 2004, 2014) or Mg/Ca measured in marine sediments (Cacho et al., 2006; Marino et al., 2013; Martinez-Mendez et al., 2010), (ii) isotopic composition of speleothems (Cheng et al., 2009; Wang et al., 2001), (iii) isotopes and greenhouse gases trapped in continental polar and tropical ice (EPICA, 2004; North Greenland Ice Core Project members, 2004; Jouzel et al., 2007; Loulerge et al., 2008; Wolff et al., 2010; Thompson et al., 1998). Diverse locations across both hemispheres, from Greenland and the North Atlantic through South America and Antarctica, among others, record these abrupt climate changes. Hence, there is currently little doubt that the Atlantic has experienced changes from warm to cold conditions and vice-versa in sub-millennial time-scale events (Barker et al., 2011) which punctuated the orbital-driven glacial-to-interglacial evolution (Berger, 1978; Jouzel et al., 2007).

Variability in the Atlantic Meridional Overturning Circulation (AMOC) is detected as one of the primary causes of these abrupt climate variations (Ganopolski and Rahmstorf, 2001; Gherardi et al., 2009; Hendy et al., 2002). In the past, AMOC reductions brought about a decrease in the transfer of heat to northern latitudes, with climate switching from warm to cold stadial modes and the consequent extension of continental and sea ice (Lippold et al., 2012; Robinson et al., 2005). While freshwater input into the North Atlantic due to melting of North American lakes may have contributed to the onset of some of these episodes (Broecker and Hemming, 2001; Teller et al., 2002), changes in the amount of salt reaching the North Atlantic as a result of variations in leakage from the Indian Ocean may have also influenced AMOC dynamics (Knorr and Lohmann, 2003; Weijer et al., 2002). Additionally, modulation of bipolar seesaw mechanisms leading to North Atlantic deep water formation, either from Arctic or

Antarctic sources, may have also had an effect on overall AMOC variability (Knorr and Lohmann, 2003; Knutti et al., 2004; Lippold et al., 2012; Martrat et al., 2007; McManus et al., 2004; Ritz et al., 2013; Stocker, 1998; Stocker and Marchal, 2000; Stocker and Johnsen, 2003; Weaver et al., 2003).

These processes draw scenarios in which abrupt climate variability responds to changes occurring at polar latitudes, whether northern or southern. Most of the evidence to explain Atlantic climate processes has been obtained from sediment cores located at mid-to-high latitudes (Allen et al., 1999; Bond et al., 1993; Martrat et al., 2007; McManus et al., 2004; Shackleton et al., 2000). However, several aspects of these changes are as yet to be explored, among them, the occurrence of abrupt climate transitions in tropical latitudes (Seager and Battisti, 2007). Climate changes in tropical Atlantic regions have received less attention, particularly those encompassing variability beyond the last deglaciation, e.g. Dubois et al. (2014), Herbert and Schuffert (2000), Jaeschke et al. (2007), Keigwin and Boyle (1999), Schmidt et al. (2004). Relevant topics for consideration are (i) identification of climate processes leading to rapid changes, (ii) detection of feedback mechanisms involved in the polar-to-tropical transmission of high latitude abrupt climate signals without loss of intensity, (iii) evaluation of the potential role of atmospheric/oceanic reorganisations in sustaining this variability. These questions require investigation into whether the tropics, as the main global store of heat and salt, may have also played an active role in abrupt climate change development or at least contributed to several stages of the process. This justifies wider exploration of the less studied tropical areas, going into greater detail as to the origin and geographic impact of rapid climate variability (Broecker, 2006).

The Guiana basin belongs to a tropical region confined between Arctic and Antarctic oceanographic influence. Its hydrography is modulated by the water discharges of the Amazon river and oscillations of the intertropical convergence zone (ITCZ). These oscillations modify winds and ocean currents, and eventually salinity, river run-off and nutrient supply (Fig. 1). This area has strategic potential for understanding what latitudinal processes have been relevant to tropical areas and which were predominant during

CPD
11, 1143–1175, 2015

the glacial and interglacial periods. In turn, changes in this tropical region could also bear an influence on Arctic regions. Given that the Guiana Current (GC) is part of the wider system transporting high saline waters from the Indian Ocean to the Caribbean Sea, changes in intensity of this current may lead to an accumulation of salt in the tropical North Atlantic. These accumulation processes may ultimately modify the density of high-latitude surface waters and the North Atlantic climate because of their influence on thermohaline circulation (Schmidt et al., 2004; Ritz et al., 2013).

Alkenones synthesized by haptophyte algae have been very successful for SST monitoring, particularly in the Atlantic Ocean (Jaeschke et al., 2007; Martrat et al., 2007; Müller et al., 1998). The alkenone unsaturation index $U^{\prime k}_{37}$ is used here to estimate SSTs (Brassell et al., 1986; Müller et al., 1998) during the past 140 ka in the western tropical Atlantic. These SST variations trace abrupt climate events and may help to identify connections with northern or southern Atlantic processes and evaluate the sensitivity of tropical areas to the changes occurring at high latitudes.

2 Regional settings

Core MD03-2616 was recovered in Guiana basin (7.4875° N, 53.0080° W by about 650 km off the coast, at 1233 m below sea level) during the PICASSO cruise on board the R/V *Marion Dufresne* (Fig. 1). The core has a total length of 39 m. Most of the sediment was formed by olive green clay, rich in foraminifera and organic matter with little bioturbation (Shipboard Scientific Party, 2003).

2.1 Atmospheric circulation

The Guiana region is situated north of South America (Fig. 1) and is directly influenced by the latitudinal migration of the ITCZ between 10° N and 5° S (Muller-Karger et al., 1989). Seasonal movements of this convergence zone generate two rainy periods (boreal late spring – early summer and winter) and two periods with less rain (boreal late summer – early autumn and early spring). This spatial and seasonal variability in the ascending branch of the Hadley cell has an impact on the vegetation and hydrology of the area, involving maximum runoff when the ITCZ is over the basins of the Amazon, Orinoco, Maroni and Oyapock rivers (Masson and Delecluse, 2001; Muller-Karger et al., 1989). Trade winds predominate in the region and change their direction depending on the ITCZ position (Fig. 1). South-east trade winds prevail when the ITCZ is in its northern position (drier continental climate; short rainfalls in Guiana). There is a predominant opposite flow of north-east trade winds when the ITCZ is in its southern position (wetter oceanic climate; long rainfalls in Guiana).

2.2 Oceanographic setting

According to the Levitus database, the present average annual at the MD03-2616 location is 27.6 °C (Reynolds et al., 2002). The GC washes the coastline from south-east to north-west (Fig. 1) and pushes the Amazon river plume towards the Caribbean Sea (Masson and Delecluse, 2001; Muller-Karger et al., 1988, 1995). This main current extends from the North Brazil Current (NBC), which branches off from the South Equatorial Current (SEC). The NBC provides salty, warm waters to the western tropical Atlantic north of the Equator (Stramma and Schott, 1999). The NBC is also influenced by the ITCZ. When the convergence zone is in its northern position it undergoes a retroflection, generating the North Equatorial Counter Current (NECC) and decreasing the GC flow. The formation and strengthening of the NBC diverts part of the Amazon plume sediment from the Caribbean Sea towards the Central Atlantic (Rühlemann et al., 2001; Zabel et al., 2003), thereby decreasing the sediment supply to the area in which core MD03-2616 is located, i.e. divergence area between the NECC and GC (Fig. 1). The Antarctic intermediate waters (AAIW) originate from subpolar latitudes around Antarctica and flow at ∼ 1000 m depth. This current can be identified in the tropical region by a salinity minimum, which contrasts with the upper North Atlantic deep-water that flows at a shallower depth than the AAIW and has higher salinity (Lankhorst et al., 2009).

CPD
11, 1143–1175, 2015

2.3 River's run off

The Amazon is the main river in South America. Its annual mean flow of 200 000 $m^3 s^{-1}$ contributes with $6 \times 10^{12} m^3 yr^{-1}$ of fresh water to the tropical Atlantic (Muller-Karger et al., 1988). Guiana's rivers (Maroni and Oyapock) have much lower runoff, 1600 and 800 $m^3 s^{-1}$, respectively, and lower influence in the area (Masson and Delecluse, 2001). The Amazon River plume is rich in nutrients and suspended sediments and forms coastal mud banks. These mud banks are associated with salinity variations and have an effect on the development of coastal ecosystems such as mangroves (Lambs et al., 2007). The material accumulated in the continental shelf is transported to the Guiana basin by the GC in a continuous band of 100–150 km. The GC carries much of the Amazon river plume northward to the Caribbean Sea (Muller-Karger et al., 1995). These river waters are rich in sediments and organic compounds generated in the Amazon forests (Saliot et al., 2001). The river is also a major contributor of nutrients to the marine system which provide appropriate habitats for algal growth, including haptophyte algae (López-Otálvaro et al., 2009).

3 Methods

3.1 Lipids and SSTs

Sediment samples (2.5 g) from MD03-2616 were taken every 3 cm. The procedure for analysis of organic compounds, including C37 alkenones, has been previously described (Villanueva and Grimalt, 1997). Briefly, samples were freeze-dried and *n*-nonadecan-1-ol, *n*-hexatriacontane and *n*-dotetracontane were added as internal standards. The sediments were then extracted with dichloromethane in an ultrasonic bath. The extracts were saponified with 10 % potassium hydroxide in methanol to eliminate interfering compounds such as fatty acids, ester waxes, aminoacids and proteins. The neutral lipid phase was recovered from this alkaline digestion with hexane, which was

CPD
11, 1143–1175, 2015

evaporated to near dryness under a gentle nitrogen stream. The lipid mixture was redissolved with toluene, derivatized with bis(trimethylsilyl) trifluoroacetamide and analyzed by gas chromatography and a flame ionisation detector (GC-FID).

Instrumental analyses were performed with a Varian 3400 equipped with a CPSIL-5 CB column coated with 100 % dimethylsiloxane (film thickness of 0.12 µm). Hydrogen was the carrier gas (50 $\mathrm{cm\,s^{-1}}$). The oven was programmed from 90 to 170 °C at 20 °C $\mathrm{min^{-1}}$, then to 280 °C at 6 °C $\mathrm{min^{-1}}$ (holding time 35 min), to 300 °C at 10 °C $\mathrm{min^{-1}}$ (holding time 7 min) and finally to 320 °C at 10 °C $\mathrm{min^{-1}}$ (holding time 3 min). The injector was programmed from 90 °C (holding time 0.3 s) to 320 °C at 200 °C $\mathrm{min^{-1}}$. The detector was maintained at 320 °C.

Selected samples were analysed by gas chromatography coupled with mass spectrometry (GC-MS; Thermo DSQ II Instruments). The instrument was equipped with a CPSIL-5 CB column and helium was used as carrier gas. Injection conditions were as described above for GC-FID. Mass spectra were acquired in the electron impact mode (70 eV) scanning from 50 to 700 mass units in cycles of 1 s.

The $U^{\prime k}_{37}$ index was obtained from the concentrations of C_{37} alkenones, $C_{37:2}/(C_{37:2}+C_{37:3})$ ($C_{37:2}$ refers to heptatriaconta-8*E*,15*E*,22*E*-trie2-one and $C_{37:3}$ to heptatriaconta-15*E*,22*E*-die2-one), and used to calculate the SST ($U^{\prime k}_{37} = 0.033 \times \mathrm{SST} + 0.044$; Müller et al., 1998).

3.2 Age model and sedimentation rates

Greenland climatic variability (Fig. 2a) and precessional oscillations (Fig. 2c) are shown as a reference for presenting the chronology applied to the MD03-2616 SSTs (Fig. 2b). From 5.9 to 34.5 ka, the MD03-2616 age-model is based on 6 AMS-^{14}C-dates measured in shelves of planktonic foraminifera *Globigerinoides sacculifer*, calibrated using the Marine13 curve (Reimer et al., 2013; Table 1). For older sections, the age model was constructed identifying the biozone with the *Y* interval of *Pulleniatina obliquiloculata* disappearance (Ericson and Wollin, 1956; Kennett and Huddlestun, 1972; Prell and Damuth, 1978; Vicalvi et al., 1999; Peterson et al., 2000; López-Otálvaro et al.,

2009) and comparing the previously published MD03-2616 benthic $\delta^{18}O_{calcite}$ determined from *Uvigerina peregrina* tests (López-Otálvaro et al., 2009; Fig. 2e) with the LR04 benthic $\delta^{18}O_{calcite}$ stack (Fig. 2d; Table 1). The LR04 stack relies on a non-linear model of ice volume, which simulates the response of ice sheets to boreal summer insolation variations (Lisiecki and Raymo, 2005).

MD03-2616 SSTs display a well-defined orbital modulation of glacial and interglacial reference marine isotope stages (MIS): the last interglacial complex MIS5e-a (from 127.3 to 71.6 ka BP), glacial stages from MIS4 to MIS2 (from 71.6 ka to 11.5 BP) and the present interglacial or MIS1 (from 11.5 to 0 ka BP). Sedimentation rates over time in Guiana (Fig. 2f) are supposed to be influenced by the sediment output of the Amazon river. The chronology used suggests that during MIS4 and MIS3 much of the sediment discharged remained in the Amazon fan and the sedimentary particle flow arriving in the Guiana basin was relatively small, average of 8 cm ka^{-1}. Apparently, sedimentation rates during the last interglacial complex (MIS5d-a) and deglacial events (late MIS2) showed higher values ranging from 4 to 30 cm^2 ka^{-1}.

4 Results

4.1 SST glacial/interglacial patterns

Alkenone-derived SSTs range from a minimum of 25.1 °C during MIS2 to a maximum of 28.9 °C in MIS5e (Fig. 2b). SST glacial-to-interglacial amplitude may appear subtle (3.8 °C), though it is in line with SSTs observed in other tropical areas such as southern China, 2.8 °C (8° N; Pelejero et al., 1999), north-eastern Brazil, 2.8 °C (4° S; Jaeschke et al., 2007) and the eastern Pacific warm pool, 2.7, 4.2 and 4 °C at 7° N, 0° N and 1° S, respectively (Dubois et al., 2014). Similarly to these previous studies, the MD03-2616 glacial-to-interglacial SST amplitude constitutes the highest SST difference observed in the interval studied, well above any other SST change associated with the rapid oscillations recorded. The top of the core contains MIS1 strata (latest dated sample at 5.9 ka BP) and averages 28.3 °C, i.e. lower SSTs than during MIS5e (Fig. 2b). MIS2 stands out as the coldest interval. Sub-stages MIS5d and MIS5b are identified from the decrease in SST to 26.7 °C. MIS4 SSTs were colder than in MIS3, down to 25.8 °C, and up to 27.7 °C, respectively. Average SST during MIS3 (26.7 °C) was higher than MIS2 and MIS4 (26.1 °C, and 26.5 °C, respectively).

Trends between perihelion passage in the NH summer and winter solstices are shown as follows (Fig. 2a and b): oscillations at warming in red (in Guiana, MIS3 and late MIS2; in Greenland, MIS5b and late MIS2), changes at cooling in blue (in Guiana, MIS 5e-a, MIS4 and early MIS2; in Greenland, MIS5d-c, and from MIS5a to MIS3) and, finally, trends of less than 1 % of the maximum change in yellow (in Greenland, early MIS2). During the last two interglacials (MIS1 and MIS5e) and warm long interstadials (MIS5d-a), both Greenland and Guiana experienced parallel cooling trends (Fig. 2a and b). SSTs around MIS5b (82.7 ka) present inverse long-term trends between Greenland and Guiana: polar latitudes showed a warming while the tropical site experienced a cooling. This is interesting, given that MIS5b comprises one of the most extreme events recorded in southern European pollen sequences (Tzedakis et al., 2003), in line with the maximum extension of the Barents-Kara and Scandinavian ice sheets (Ehlers et al., 2011) which blocked drainage of north-east European rivers owing to large proglacial lakes (Krinner et al., 2004). Additionally, note the opposite trends between Guiana and Greenland during MIS3 and early MIS2 (Table 2 includes rates of Change and number of samples used).

4.2 Abrupt SST changes

Sub-millennial-scale rapid variations during the last climate cycle have been documented in Greenland ice (North Greenland Ice Core Project members, 2004; Wolff et al., 2010; Figs. 3a and 4a). MD03-2616 SSTs showed a remarkable parallelism with temperature changes observed in Greenland during the last two interglacials (MIS1 and MIS5e) and warm long interstadials (MIS5d-a). From MIS4 to MIS2, the Dansgaard–Oeschger type of oscillations form the background of the climate variability

CPD
11, 1143–1175, 2015

observed (Figs. 3b and 4b). SST changes contain strong precessional climatic modulation (Figs. 3c and 4c). The overall MD03-2616 SST profile shows a maximum fall of −2.2 °C, i.e. less than those observed in the North Atlantic, e.g. −10 °C in the Iberian Margin (Bard et al., 2000; Martrat et al., 2007) or −6 °C in the Alboran Sea (Martrat et al., 2004; Cacho et al., 1999). Lesser amplitudes in MD03-2616 are consistent with the narrower SST range found in tropical regions. Previous studies identified abrupt changes based on the fastest rate of change associated with the last deglaciation (Martrat et al., 2004; Rahmstorf, 2003). In Guiana, this interval presents a rate of change of +2 °C ka^{-1} (3.1 °C in 1550 years in the MD03-2616 record; Fig. 3b; Table 3). Thus, in this study, events with a warming/cooling speed higher than ±0.5 and ±2 °C ka^{-1} were considered abrupt. Most events were found in the glacial period when instability was higher (Fig. 3b). Some relevant SST oscillations are detected at transitional phases such as MIS5d (+2.0 °C), MIS5b (up to +3.5 °C), MIS4 (−3.5 °C), during early MIS3 (+2.2 °C), early MIS2 (e.g. +5.1 °C or −3.3 °C) or around the events known as Bølling–Allerød (B-A) and the Younger Dryas (YD) in a North Atlantic context (Figs. 3b and 4b; Table 3).

The intra-MIS5e variability previously reported in the North Atlantic (Oppo et al., 2001, 2006) is also observed in Guiana (Fig. 4b). From MIS5c to MIS5a (GS and GI from 25 to 19), SSTs followed a pace of events similar to those of Greenland. Generally, SST oscillations did not exceed 0.5 °C, though some remarkable exceptions are observed around GS-24 (cold event C23 in McManus et al., 1994, 2002), GS-22 (cold event C21 in McManus et al., 1994, 2002) and GS-25 (cold event C24 in McManus et al., 1994, 2002). Transitions from MIS5a to MIS4 and from MIS3 to MIS2 were abrupt (e.g. cooling of −1.5 °C in 0.4 ka; Table 3) and presented high instability, i.e. warming and cooling events occurred rapidly (in less than 1.5 ka). The MIS3 transition started with a rapid warming at 57 ka (+1.4 °C in 0.6 ka) and exhibited high Variability (Fig. 3b). Late MIS2 presents a warming trend (Fig. 2b; Table 2), interrupted by cooling episodes at 17.5 ka (ca. −1.4 °C) and by around 12 ka (e.g. −2.2 °C in 0.4 ka) which could cor-

CPD
11, 1143–1175, 2015

respond to the stadials associated with Heinrich event 1 (H1) and the YD respectively, as described at higher latitudes (Fig. 3b).

5 Discussion

5.1 Rapid tropical-pole connections during warm, stable periods

The fact that SSTs in MIS5e (28.9 °C) are higher than in the MIS1 (28.3 °C) further confirms previous observations which suggest a remarkable precessional modulation behind the differences between both interglacials (e.g. Martrat et al., 2014) (Figs. 3b and 4b). Prominent drops in SST around MIS5d and MIS5b, features characteristic in the North Atlantic, occurred after precessional maxima (insolation minima; Fig. 4c). Specifically, prolonged interglacial warmth in the North Atlantic after insolation minima (116.3 ka; Table 2) has been attributed to a strengthening in thermohaline circulation (McManus et al., 2002). High latitude climate changes in the Northern Hemisphere were transmitted towards the southern Atlantic Ocean even at latitudes of 7° N during periods when precessional changes increased in amplitude. When the transport of salt from the Caribbean Sea to North Atlantic latitudes was strong and the AMOC was active, close connection between high latitudes and tropical regions was enabled.

During the latest stages of the last deglaciation, MD03-2616 SSTs are a reminder of oscillations observed in Greenland (North Greenland Ice Core Project members, 2004), with structures similar to the B-A and the stadial associated with H1 respectively (Fig. 3a and b). Once again, these SST changes were of lesser intensity in the Guiana core than in the North Atlantic, consistent with the common subdued SST variability in tropical regions. Concerted changes between Guiana and Greenland during the last deglaciation suggest that the advection of salty warm tropical waters into the North Atlantic amplified thermohaline circulation and contributed to high-latitude warming (Knorr and Lohmann, 2003; Schmidt et al., 2004).

CPD
11, 1143–1175, 2015

Possible links between the MD03-2616 SST record and those from the cores in the Agulhas area should be considered, given that the Guiana core is located in the area of influence of the NBC originating from the SEC and providing salty warm waters to the western tropical Atlantic north of the equator (Fig. 1; Stramma and Schott, 1999). The SEC is ultimately fed by leakage from the Agulhas current (Bard and Rickaby, 2009; Caley et al., 2014; Dyez et al., 2014). Intensification in the delivery of salt into the Atlantic may contribute to strengthening the AMOC flow. Hydrographical changes in equatorial currents have previously been put forward as a possible influence on the development and intensity of interglacial SSTs (Ganachaud and Wunsch, 2000; Trenberth and Caron, 2001). However, SST reconstructions influenced by the Agulhas current (Martinez-Mendez et al., 2010; Marino et al., 2013; Dyez et al., 2014; Bard and Rickaby, 2009) differ from the MD03-2616 SST record (not shown).

Conversely, the coupling between SST change in MD03-2616, the Greenland temperatures and the SST of northern Atlantic latitudes in the interglacials is consistent with the model describing an AMOC dependence on global mean air temperature anomalies and North Atlantic SSTs (Ritz et al., 2013). Analogous SST evolution between tropical areas and Greenland suggests that ocean processes in Guiana are directly related to the AMOC strength during the last two interglacials (MIS5e and MIS1) and warm long interstadials (MIS5d-a). This parallel behaviour is in line with the amplification of thermohaline circulation resulting from the movement of salty tropical waters into the North Atlantic, as observed in cores from the Caribbean Sea (12° N, 78° W; Schmidt et al., 2004). The coupling of the west tropical Atlantic waters with these processes was probably necessary for the supply of salty waters to the Caribbean Sea prior to concentration and advection towards the North Atlantic. The coupling is observed irrespectively of the higher amounts of sediment from the Amazon river discharged into MD03-2616 during the interglacials. Possible local effects caused by Amazon discharges in this area did not significantly disturb the MD03-2616 SST record, which preserves a remarkable parallelism between tropical climate changes and Greenland variability.

CPD
11, 1143–1175, 2015

5.2 Tropical abrupt SST changes during transitional intervals

While, in the North Atlantic, abrupt changes occurred throughout MIS3 (Martrat et al., 2004), in MD03-2616 they are mostly to be found at the end of this stage. Hence, most abrupt changes occur during deglaciation periods (Fig. 3b; Table 3). This pattern is somewhat consistent with the events described above. When the AMOC is active, the climate also undergoes abrupt variability. In this respect, MD03-2616 exhibits abrupt oscillations around the B-A. This feature has also been observed in the $\delta^{18}O_{ice}$ record of continental ice accumulated in Sajama (Bolivia; Thompson et al., 1998), which reinforces the evidence of links between the climate changes in the North Atlantic and in central and south America during the end of the last deglaciation (Fig. 3a and b).

A strong SST variability in the YD has been identified in core MD03-2616. Bearing in mind that the YD most likely resulted from the massive discharge of cold freshwater into the North Atlantic, causing a decrease in the AMOC (Broecker and Hemming, 2001; Teller et al., 2002), it is feasible that such huge freshwater inputs could modify oceanic circulation in the tropical Atlantic. The influence of these northern waters may have had an effect on latitudinal displacements of the ITCZ which may have also resulted in SST variations in Guiana. The onset of this cold period was very abrupt at the Guiana site, with SST decreases of ca. $-6\,^{\circ}\mathrm{C\,ka^{-1}}$ and changes over $2\,^{\circ}\mathrm{C}$ (Table 3).

During glacial periods, the SST record of MD03-2616 shows significant variability, with oscillations of 0.5–1.2 °C. This represents about 30 % of the maximum SST change during the glacial to interglacial transition or vice versa (3.8 °C). This relative change is lower than that observed in more northern sites of the North Atlantic, such as Blake Outer Reach (50 % in ODP-1060; López-Martinez et al., 2006), the Iberian Margin (46 % in MD01-2044; Martrat et al., 2007) or the Alboran Sea (40 % in ODP-977; Martrat et al., 2004 or 46 % in MD95-2043; Cacho et al., 1999). The sub-millennial variability of MD03-2616 in MIS3 is therefore lower than in the cores retrieved further north in the North Atlantic. Changes at high latitudes are stronger than in the tropics due to sea-ice albedo feedbacks (Menviel et al., 2014). In this respect, it is hard to identify unambiguously either the Dansgaard-Oeschger type of oscillations described in northern latitudes or the SST drops associated with the Heinrich events characterising North Atlantic records.

5.3 Glacial see-saw between the tropics and Greenland

Previously published datasets are available to assess the significance of trends and events observed in Greenland and in Guiana during the glacial (Fig. 5a and b). Long term trends in the ODP 1002C reference core from the Cariaco basin (ca. 72 radiocarbon dates; 10° N, 65° W; Peterson et al., 2000) are in line with the trends observed in Guiana for the time span in which they overlap (Fig. 5c). The nearby core MD03-2622 (10° N, 65° W; Gonzalez et al., 2008) documents vegetation patterns consistent with the rapid variability of Greenland. Similarly, the extent to which the well-dated SST record in GeoB 3910-2 (Jaeschke et al., 2007) agrees with the trends observed in Guiana supports that these tropical cores present reminders of Greenland rapid oscillations but also a robust response to precessional forcing (Fig. 5d). Terrestrial records of Central America from Lake Peten Itza (Guatemala, 17° N, 89° W) also follow the MIS3 abrupt variability recorded in Greenland ice (Hodell et al., 2008). Cold conditions over the North Atlantic and strong trades induce a southward shift of the ITCZ over the Atlantic region with hydrological perturbations simulated over the northern part of South America (Menviel et al., 2014). The same is the case for terrestrial climate signals involving contributions from pollen, fern spores and lithogenic deposition (e.g. Ti/Ca or Fe/Ca ratios, or continental organic matter inputs) in Brazilian cores, which follow sedimentation pulses paralleling those recorded during Heinrich events (Jennerjahn et al., 2004; Nace et al., 2014). Hence, the influence of abrupt climate variations in the North Atlantic and Greenland encompassed a large extension of tropical regions. This evidence suggests that the marine and continental climate of northern South America connected with polar variability during glacial periods, though reacting in a muted way and mainly dominated by precessional forcing.

Lack of synchrony between trends in tropical SST records and Greenland temperatures are also observed in high resolution profiles from sites located in the Agulhas current (not shown), such as in cores MD96-2080 (Simon et al., 2013) and MD02-2594 (Dyez et al., 2014) or tropical cores located in the eastern Atlantic (Gulf of Guinea, 2° N, 9° E; Weldeab et al., 2007). SST dynamics of these sites have been attributed to poleward displacements of the subtropical front of the Southern Hemisphere which coincides with warm intervals south of Africa in the western Atlantic Ocean (De Dekker et al., 2012). Nevertheless, the lack of consistent SST change in MD03-2616 and the cores in the Agulhas area or the northeastern tropical Atlantic during the last glacial period (Zarries et al., 2011) evidence the long-term trend decoupling between these geographic areas during low intensity of the AMOC.

6 Conclusions

SSTs in the western tropical Atlantic (MD03-2616; Guiana basin) over the past 140 ka ranged from 25.1 °C (MIS2) to 28.9 °C (MIS5e), i.e. a glacial–interglacial amplitude of SST variations was 3.8 °C, in the same range as those observed in other tropical areas. SSTs during the MIS1 (28.3 °C) were lower than in MIS5e, which is consistent with observations from previous studies at North Atlantic latitudes. MIS5b and MIS5d decreases are much smaller than those observed in the Atlantic Ocean at higher latitudes, though proportional to the subdued glacial-to-interglacial SST range of tropical regions.

From MIS5e to MIS5a, SSTs in Guiana show a remarkable parallelism with the temperature changes observed in Greenland, suggesting a close connection between tropical and arctic Atlantic latitudes in these periods. A possible mechanism to explain this connection is the transport of salt from the Caribbean Sea to North Atlantic latitudes when the whole AMOC was active and strong, thereby facilitating the thermohaline transmission role resulting from the transfer of salty tropical waters into the North Atlantic.

Abrupt transitions have been identified in core MD03-2616. Some of these changes are observed in MIS5d and MISb but are much more commonly found during transitional periods from MIS4 to MIS2. The influence of northern waters during deglaciation periods may have had an effect on the latitudinal displacements of the ITCZ, which could also have increased SST variability in Guiana. MD03-2616 SSTs exhibit a strong abrupt warming and cooling changes coincident with the B-A. This variability has also been observed in the $\delta^{18}O_{ice}$ profile of Sajama, a Bolivian ice core. Both sites show a very abrupt end of the YD (rates of 4 °C ka^{-1} and more than a 2.5 °C change in MD03-2616).

MD03-2616 SSTs show significant variability in large sections of MIS3, comprising oscillations of 0.5–1.2 °C, representing about 30 % of the maximum glacial–interglacial SST change of 3.8 °C. This change is lower than that of the northern North Atlantic. During MIS3 and early MIS2, the SST record in Guiana appears to balance changes in the characteristic long-term trend observed at higher latitudes. When Greenland experienced a cooling trend, Guiana showed a warming; or vice versa, Greenland remained stable when Guiana experienced a cooling trend. This lack of synchrony is consistent with SST records in northern and southern locations of the Atlantic Ocean (Cariaco and Brazil, respectively) and evidence the decoupling between these areas when the AMOC weakens.

Acknowledgements. The work presented here has been co-funded by research projects GRACCIE (CSD2007-00067, Programa Consolider-Ingenio 2010) and Past4Future (FP7-ENV-2009-1-243908. Contribution no 86). B. Martrat thanks CSIC-JAE-Doc and Ramon y Cajal post-doctoral contracts. The IMAGES Program and the scientific and technical cruise of the PICASSO expedition on board the R/V *Marion Dufresne* II are thanked for their efforts in the retrieval of core MD03-2616. We are also grateful to the Latin-American Abrupt Climate changes and Environmental Responses (LaACER) initiative.

CPD
11, 1143–1175, 2015

Parallelisms between sea surface temperature changes in the western tropical Atlantic

O. Rama-Corredor et al.

References

Allen, J. R. M., Brandt, U., Brauer, A., Hubberten, H.-W., Huntley, B., Kellerk, J., Kramlk, M., Mackensen, A., Mingram, J., Negendank, J. F. W., Nowaczyk, N. R., Oberhansli, H. Watts, W. A., Wulf, S., and Zolitschka, B.: Rapid environmental changes in southern Europe during the last glacial period, Nature, 400, 740–743, 1999.

Bard, E. and Rickaby, E. M.: Migration of the subtropical front as a modulator of glacial climate, Nature, 460, 380–384, 2009.

Bard, E., Rostek, F., and Ménot-Combes, G.: Radiocarbon calibration beyond 20 000 ^{14}C yr BP by means of planktonic foraminifera of the Iberian Margin, Quaternary Res., 61, 204–214, 2004.

Barker, S., Knorr, G., Edwards, R. L., Parrenin, F., Putnam, A. E., Skinner, L. C., Wolff, E., and Ziegler, M.: 800 000 years of abrupt climate variability, Science, 334, 347–351, 2011.

Berger, A.: Long-term variations of daily insolation and quaternary climatic changes, J. Atmos. Sci., 35, 2362–2367, 1978.

Bond, G., Broecker, W., Johnsen, S., McManus, J., Labeyrie, L., Jouzel, J., and Bonani, G.: Correlations between climate records from North Atlantic sediments and Greenland ice, Nature, 365, 143–147, 1993.

Brassell, S. C., Eglinton, G., Marlowe, I. T., Pflaumann, U., and Sarnthein, M.: Molecular stratigraphy: a new tool for climatic assessment, Nature, 320, 129–133, 1986.

Broecker, W. S.: Was the younger dryas triggered by a flood?, Science, 312, 1146–1148, 2006.

Broecker, W. S. and Hemming, S.: Climate swings come into focus, Science, 294, 2308–2309, 2003.

Cacho, I., Shackleton, N., Elderfield, H., Sierro, F. J., and Grimalt, J. O.: Glacial rapid variability in deep water temperature and δ^{18}O from the Western Mediterranean Sea, Quaternary Sci. Rev., 25, 3294–3311, 2006.

Caley, T., Peeters, F. J. C., Biastoch, A., Rossignol, L. , van Sebille, E., Durgadoo, J., Malaizé, B., Giraudeau, J., Arthur, K., and Zahn, R.: Quantitative estimate of the paleo-Agulhas leakage, Geophysical Res. Lett., 41,doi:10.1002/2014GL059278, 2014.

Cheng, H., Edwards, R. L., Broecker, W. S., Denton, G. H., Kong, X., Wang, Y., Zhang, R., and Wang, X.: Ice Age terminations, Science, 326, 248–252, 2009.

De Dekker, P., Moros, M., Perner, K., and Jansen, E.: Influence of the tropics and southern westerlies on glacial interhemispheric asymmetry, Nat. Geosci., 5, 266–269, 2012.

CPD
11, 1143–1175, 2015

Parallelisms between sea surface temperature changes in the western tropical Atlantic

O. Rama-Corredor et al.

Dubois, N., Kienast, M., Kienast, S. S., and Timmermann, A.: Millennial-scale Atlantic/East Pacific sea surface temperature linkages during the last 100,000 years, Earth Planet. Sci., 396, 134–142, 2014.
Dyez, K. A., Zahn, R., and Hall, I. R.: Multicentennial Agulhas leakage variability and linls to north Atlantic climate during the past 800 000 years, Paleoceanography, 29, 1238–1248, doi:10.1002/2014PA002698, 2014.
Ehlers, J., Gibbard, P. L., and Hughes, P. D.: Quaternary Glaciations - Extent and Chronology, Part IV - A Closer Look. Developments in Quaternary Science. Amsterdam: Elsevier. 1,126 pages (78 Chapters)., 2011
EPICA community members: Eight glacial cycles from an Antarctic ice core, Nature, 429, 623–628, 2004.
Ericson, D. B. and Wollin, G.: Correlation of six cores from the equatorial Atlantic and the Caribbean, Deep-Sea Res., 3, 104–125, 1956.
Ganachaud, A. and Wunsch, C.: Improved estimates of global ocean circulation, heat transport and mixing from hydrographic data, Nature, 408, 453–456, 2000.
Ganopolski, A. and Rahmstorf, S.: Rapid changes of glacial climate simulated in a coupled climate model, Nature, 409, 153–158, 2001.
Gherardi, J. M., Labeyrie, L., Nave, S., Francois, R., McManus, J. F., and Cortijo, E.: Glacial–interglacial circulation changes inferred from $^{231}Pa/^{230}Th$ sedimentary record in the North Atlantic region, Paleoceanography, 24, PA2204, doi:10.1029/2008PA001696, 2009.
González, C., Dupont, L. M., Behling, H., and Wefer, G.: Neotropical vegetation response to rapid climate changes during the last glacial period: palynological evidence from the Cariaco Basin, Quaternary Res., 69, 217–230, 2008.
Hendy, I. L., Kennett, J. P., Roark, E. B., and Ingram, B. L.: Apparent synchroneity of submillennial scale climate events between Greenland and Santa Barbara Basin, California from 30–10 ka, Quaternary Sci. Rev., 21, 1167–1184, 2002.
Herbert, T. D. and Schuffert, J. D.: Alkenone unsaturation estimates of sea-surface temperatures at site 1002 over a full glacial cycle, in: Proceedings of the Ocean Drilling Program: Scientific Results, 165, 239–247, 2000.
Hodell, D. A., Anselmetti, F. S., Ariztegui, D., Brenner, M., Curtis, J. H., Gilli, A., Grzesik, D. A., Guilderson, T. J., Müller, A. D., Bush, M. B., Correa-Metrio, A., Escobar, J., and Kutterolf, S.: An 85-ka record of climate change in lowland Central America, Quaternary Sci. Rev., 27, 1152–1165, 2008.

CPD
11, 1143–1175, 2015

Parallelisms between sea surface temperature changes in the western tropical Atlantic

O. Rama-Corredor et al.

Jaeschke, A., Rühlemann, C., Arz, H., Heil, G., and Lohmann, G.: Coupling of millennial-scale changes in sea surface temperature and precipitation off northeastern Brazil with high-latitude climate shifts during the last glacial period, Paleoceanography, 22, PA4206, doi:10.1029/2006PA001391, 2007.
Jennerjahn, T. C., Ittekkot, V., Arz, H. W., Behling, H., Patzold, J., and Wefer, G.: Asynchronous terrestrial and marine signals of climate change during Heinrich Events, Science, 306, 2236–2239, 2004.
Jouzel, J., Masson-Delmotte, V., Cattani, O., Dreyfus, G., Falourd, S., Hoffmann, G., Minster, B., Nouet, J., Barnola, J. M., Chappellaz, J., Fischer, H., Gallet, J. C., Johnsen, S., Leuenberger, M., Loulergue, L., Luethi, D., Oerter, H., Parrenin, F., Raisbeck, G., Raynaud, D., Schilt, A., Schwander, J., Selmo, E., Souchez, R., Spahni, R., Stauffer, B., Steffensen, J. P., Stehni, B., Stocker, T. F., Tison, J. L., Werner, M., and Wolff, E. W.: Orbital and millennial antarctic climate variability over the past 800 000 years, Science, 317, 793–796, 2007.
Keigwin, L. D. and Boyle, E. A.: Surface and deep ocean variability in the northern Sargasso Sea during marine isotope stage 3, Paleoceanography, 14, 164–170, 1999.
Kennett, J. P. and Huddlestun, P.: Late Pleistocene paleoclimatology, foraminiferal biostratigraphy and tephrochronology, western Gulf of Mexico, Quaternary Res., 2, 38–69, 1972.
Knorr, G. and Lohmann, G.: Southern Ocean origin for the resumption of Atlantic thermohaline circulation during deglaciation, Nature, 424, 532–536, 2003.
Knutti, R., Fluckiger, J., Stocker, T. F., and Timmermann, A.: Strong hemispheric coupling of glacial climate through freshwater discharge and ocean circulation, Nature, 430, 851–856, 2004.
Krinner, G., Mangerud, J., Jakobsson, M., Crucifix, M., Ritz, C., and Svendsen, J. I.: Enhanced ice sheet growth in Eurasia owing to adjacent ice-dammed lakes, Nature, 427, 429–432, 2004.
Lambs, L., Müller, E., and Fromard, F.: The Guianese Paradox: how can the freshwater outflow from the Amazon increase the salinity of the Guianan shore?, J. Hydrol., 342, 88–96, 2007.
Lankhorst, M., Fratantoni, D., Ollitrault, M., Richardson, P., Send, U., and Zenk, W.: The mid-depth circulation of the northwestern tropical Atlantic observed by floats, Deep-Sea Res. Pt. I, 56, 1615–1632, 2009.
Lippold, J., Luo, Y., François, R., Allen, S. E., Gherardi, J., Pichat, S., Hickey, B., and Schulz, H.: Strength and geometry of the glacial Atlantic Meridional Overturning Circulation, Nat. Geosci., 5, 813–816, 2012.

Lisiecki, L. E. and Raymo, M. E.: A Pliocene-Pleistocene stack of 57 globally distributed benthic δ^{18}O records, Paleoceanography, 20, PA1003, doi:10.1029/2004PA001071, 2005.
López-Martínez, C., Grimalt, J. O., Hoogakker, B., Gruetzner, J., Vautravers, M. J., and McCave, I. N.: Abrupt wind regime changes in the North Atlantic Ocean during the past 30 000–60 000 years, Paleoceanography, 21, PA4215, doi:10.1029/2006PA001275, 2006.
López-Otálvaro, G.-E., Flores, J. A., Sierro, F. J., Cacho, I., Grimalt, J.-O., Michel, E., Cortijo, E., and Labeyrie, L.: Late Pleistocene palaeoproductivity patterns during the last climatic cycle in the Guyana Basin as revealed by calcareous nannoplankton, eEarth, 4, 1–13, doi:10.5194/ee-4-1-2009, 2009.
Loulergue, L., Schilt, A., Spahni, R., Masson-Delmotte, V., Blunier, T., Lemieux, B., Barnola, J.-M., Raynaud, D., Stocker, T. F., and Chappellaz, J.: Orbital and millennial-scale features of atmospheric CH_4 over the past 800 000 years, Nature, 453, 383–386, 2008.
Marino, G., Zahn, R., Ziegler, M., Purcell, C., Knorr, G., Hall, I. R., Ziveri, P., and Elderfield, H.: Agulhas salt-leakage oscillations during abrupt climate changes of the late Pleistocene, Paleoceanography, 28, 599–606, 2013.
Martinez-Mendez, G., Zahn, R., Hall, I. R., Peeters, F. J. C., Pena, L. D., Cacho, I., and Negre, C.: Contrasting multiproxy reconstructions of surface ocean hydrography in the Agulhas Corridor and implications for the Agulhas leakage during the last 345 000 years, Paleoceanography, 25, PA4227, doi:10.1029/2009PA001879, 2010.
Martrat, B., Grimalt, J. O., Lopez-Martinez, C., Cacho, I., Sierro, F. J., Flores, J. A., Zahn, R., Canals, M., Curtis, J. H., and Hodell, D. A.: Abrupt temperature changes in the Western Mediterranean over the past 250 000 years, Science, 306, 1762–1765, 2004.
Martrat, B., Grimalt, J. O., Shackleton, N. J., De Abreu, L., Hutterli, M. A., and Stocker, T. F.: Four climate cycles of recurring deep and surface water destabilizations on the Iberian margin, Science, 317, 502–507, 2007.
Martrat, B., Jimenez-Amat, P., Zahn, R., and Grimalt, J. O.: Similarities and dissimilarities between the last two deglaciations and interglaciations in the North Atlantic region, Quaternary Sci. Rev., 99, 122–134, 2014.
Masson, S. and Delecluse, P.: Influence of the Amazon river runoff on the tropical atlantic, Phys. Chem. Earth Pt. B, 26, 137–142, 2001.
McManus, J. F., Francois, R., Gherardi, J.-M., and Keigwin, L. D.: Collapse and rapid resumption of Atlantic meridional circulation linked to deglacial climate changes, Nature, 428, 834–837, 2004.

CPD
11, 1143–1175, 2015

Parallelisms between sea surface temperature changes in the western tropical Atlantic

O. Rama-Corredor et al.

McManus, J. F., Bond, G. C., Broecker, W. S., Johnsen, S., Labeyrie, L., and Higgins, S.: High-resolution climate records from the North Atlantic during the last interglacial, Nature, 371, 326–329, 1994.
McManus, J. F., Oppo, D. W., Keigwin, L. D., Cullen, J. L., and Bond, G. C.: Thermohaline circulation and prolonged interglacial warmth in the North Atlantic, Quaternary Res., 58, 17–21, 2002.
Menviel, L., Timmermann, A., Friedrich, T., and England, M. H.: Hindcasting the continuum of Dansgaard–Oeschger variability: mechanisms, patterns and timing, Clim. Past, 10, 63–77, doi:10.5194/cp-10-63-2014, 2014.
Muller-Karger, F. E., McClain, C. R., and Richardson, P. L.: The dispersal of the Amazon's water, Nature, 333, 56–59, 1988.
Muller-Karger, F. E., McClain, C. R., Fisher, T. R., Esaias, W. E., and Varela, R.: Pigment distribution in the Caribbean sea: observations from space, PrOce, 23, 23–64, 1989.
Muller-Karger, F. E., Richardson, P. L., and McGillicuddy, D.: On the offshore dispersal of the Amazon's Plume in the North Atlantic: comments on the paper by A. Longhurst, "Seasonal cooling and blooming in tropical oceans", Deep-Sea Res. Pt. I, 42, 2127–2131, 1995.
Müller, P. J., Kirst, G., Ruhland, G., Von Storch, I., and Rosell-Mele, A.: Calibration of the alkenone paleotemperature index U37 K based on core-tops from the eastern South Atlantic and the global ocean (60° N–60° S), Geochim. Cosmochim. Ac., 62, 1757–1772, 1998.
Nace, T. E., Baker, P. A., Dwyer, G. S., Silva, C. G., Rigsby, C. A., Burns, S. J., Giosan, L., Otto-Bliesner, B., Liu, Z., and Zhu, J.: The role of North Brazil current transport in the paleoclimate of the Brazilian Nordeste margin and paleoceanography of the western tropical Atlantic during the late Quaternary, Palaeogeogr. Palaeocl., 415, 3–13, 2014.
NEEM community members: Eemian interglacial reconstructed from a Greenland folded ice core, Nature, 493, 489–494, 2013.
North Greenland Ice Core Project members: High-resolution record of Northern Hemisphere climate extending into the last interglacial period, Nature, 431, 147–151, 2004.
Oppo, D. W., Keigwin, L. D., McManus, J. F., and Cullen, J. L.: Persistent suborbital climate variability in marine isotope stage 5 and termination II, Paleoceanography, 16, 280–292, 2001.
Oppo, D. W., McManus, J. F., and Cullen, J. L.: Evolution and demise of the Last Interglacial warmth in the subpolar North Atlantic, Quaternary Sci. Rev., 25, 3268–3277, 2006.

Pelejero, C., Grimalt, J. O., Sarnthein, M., Wang, L., and Flores, J.-A.: Molecular biomarker record of sea surface temperature and climatic change in the South China Sea during the last 140 000 years, Mar. Geol., 156, 109–121, 1999.

Peterson, L. C., Haug, G. H., Hughen, K. A., and Rohl, U.: Rapid changes in the hydrologic cycle of the tropical Atlantic during the Last Glacial, Science, 290, 1947–1951, 2000.

Prell, W. L. and Damuth, J. E.: The climate-related diachronous disappearance of *Pulleniatina obliquiloculata* in late quaternary sediments of the Atlantic and Caribbean, Mar. Micropaleontol., 3, 267–277, 1978.

Reimer, P. J., Bard, E., Bayliss, A., Beck, J. W., Blackwell, P. G., Bronk Ramsey, C., Buck, C. E., Cheng, H., Edwards, R. L., Friedrich, M., Grootes, P. M., Guilderson, T. P., Haflidason, H., Hajdas, I., Hatté, C., Heaton, T. J., Hoffmann, D. L., Hogg, A. G., Hughen, K. A., Kaiser, K. F., Kromer, B., Manning, S. W., Niu, M., Reimer, R. W., Richards, D. A., Scott, E. M., Southon, J. R., Staff, R. A., Turney, C. S. M., and van der Plicht, J.: IntCal13 and Marine13 Radiocarbon Age Calibration Curves 0–50 000 Years cal BP, Radiocarbon, 55, 1869–1887, 2013.

Reynolds, R. W., Rayner, N. A., Smith, T. M., Stokes, D. C., and Wang, W.: An improved in situ and satellite SST analysis for climate, J. Climate, 15, 1609–1625, 2002.

Ritz, S. P. Stocker, T. F., Grimalt, J. O., Menviel, L., and Timmermann, A.: Estimated strength of the Atlantic overturning circulation during the last deglaciation, Nat. Geosci., 6, 208–212, 2013.

Robinson, L. F., Adkins, J. F., Keigwin, L. D., Southon, J., Fernandez, D. P., Wang, S.-L., and Scheirer, D. S.: Radiocarbon variability in the western north Atlantic during the last deglaciation, Science, 310, 1469–1473, 2012.

Rühlemann, C., Diekmann, B., Mulitza, S., and Frank, M.: Late Quaternary changes of western equatorial Atlantic surface circulation and Amazon lowland climate recorded in Ceará Rice deep-sea sediments, Paleoceanography, 16, 293–305, 2001.

Saliot, A., Mejanelle, L., Scribe, P., Fillaux, J., Pepe, C., Jabaud, A., and Dagaut, J.: Particulate organic carbon, sterols, fatty acids and pigments in the Amazon River system, Biogeochemistry, 53, 79–103, 2001.

Schmidt, M. W., Spero, H. J., and Lea, D. W.: Links between salinity variation in the Caribbean and North Atlantic thermohaline circulation, Nature, 428, 160–163, 2004.

CPD

11, 1143–1175, 2015

Seager, R. and Battisti, D. S.: Challenges to our understanding of the general circulation: abrupt climate change, in: Global Circulation of the Atmosphere, edited by: Schneider, T. and Sobel, S., Princenton University Press, 331–337, 2007.
Shackleton, N. J., Hall, M. A., and Vincent, E. Phase relationships between millennial-scale events 64 000–24 000 years ago, Paleoceanography, 15, 565–569, 2000.
Shipboard Scientific Party: Shipboard Scientific Party MD132-PICASSO, IMAGES XI Cruise Report, 76, 2003.
Stocker, T. F.: The Seesaw Effect, Science, 282, 61–62, 1998.
Stocker, T. F. and Johnsen, S. J.: A minimum thermodynamic model for the seesaw, Paleoceanography, 18, PA1087, doi:10.1029/2003PA000920, 2003.
Stocker, T. F. and Johnsen, S. J.: Correction to “A minimum thermodynamic model for the bipolar seesaw”, Paleoceanography, 20, PA1002, doi:10.1029/2004PA001108, 2005.
Stocker, T. F. and Marchal, O.: Abrupt climate change in the computer: is it real?, P. Natl. Acad. Sci. USA, 97, 1362–1365, 2000.
Stramma, L. and Schott, F.: The mean flow field of the tropical Atlantic Ocean, Deep-Sea Res. Pt. II, 46, 279–303, 1999.
Teller, J. T., Leverington, D. W., and Mann, J. D.: Freshwater outbursts to the oceans from glacial Lake Agassiz and their role in climate change during the last deglaciation, Quaternary Sci. Rev., 21, 879–887, 2002.
Thompson, L. G., Davis, M. E., Mosley-Thompson, E., Sowers, T. A., Henderson, K. A., Zagorodnov, V. S., Lin, P.-N., Mikhalenko, V. N., Campen, R. K., Bolzan, J. F., Cole-Dai, J., and Francou, B.: A 25 000-year tropical climate history from Bolivian ice cores, Science, 282, 1858–1864, 1998.
Trenberth, K. E. and Caron, J. M.: Estimates of meridional atmosphere and ocean heat transports, J. Climate, 14, 3433–3443, 2001.
Tzedakis, P. C., McManus, J. F., Hooghiemstra, H., Oppo, D. W., and Wijmstra, T. A.: Comparison of changes in vegetation in northeast Greece with records of climate variability on orbital and suborbital frequencies over the last 450 000 years, Earth Planet. Sc. Lett., 212, 197–212, 2003.
Vicalvi, M. A.: Zoneamento bioestratigráfico e paleoclimático do quaternário superior do talude da Bacia de Campos e platô de São Paulo adjacente, com base em foraminíferos planctônicos, Anu. Inst. Geocienc, 22, 117–119, 1999.

CPD
11, 1143–1175, 2015

Parallelisms between sea surface temperature changes in the western tropical Atlantic

O. Rama-Corredor et al.

Villanueva, J. and Grimalt, J. O.: Gas chromatographic tuning of the Uk'37 paleothermometer, Anal. Chem., 69, 3329–3332, 1997.
Wang, Y. J., Cheng, H., Edwards, R. L., An, Z. S., Wu, J. Y., Shen, C.-C., and Dorale, J. A.: A high-resolution absolute-dated late Pleistocene monsoon record from Hulu Cave, China, Science, 294, 2345–2348, 2001.
Weaver, A. J., Saenko, O. A., Clark, P. U., and Mitrovica, J. X.: Meltwater pulse 1A from Antarctica as a trigger of the Bølling–Allerød warm interval, Science, 299, 1709–1713, 2003.
Weijer, W., De Ruijter, W. P. M., Sterl, A., and Drijfhout, S. S.: Response of the Atlantic overturning circulation to South Atlantic sources of buoyancy, Global Planet. Change, 34, 293–311, 2002.
Weldeab, S., Schneider, R. R., and Müller, P.: Comparison of Mg/Ca- and alkenone-based sea surface temperature estimates in the fresh water-influenced Gulf of Guinea, eastern equatorial Atlantic, Geochem. Geophy. Geosy., 8, Q05P22, doi:10.1029/2006GC001360, 2007.
Wolff, E. W., Chappellaz, J., Blunier, T., Rasmussen, S. O., and Svensson, A.: Millennial-scale variability during the last glacial: the ice core record, Quaternary Sci. Rev., 29, 2828–2838, 2010.
Zabel, M., Wagner, T., and de Menocal, P.: Terrigenous Signals in Sediments of the Low-Latitude Atlantic – Indications to Environmental Variations during the Late Quaternary: Part II: Lithogenic Matter, in: The South Atlantic in the Late Quaternary, edited by: Wefer, G., Mulitza, S., and Ratmeyer, V., Springer Berlin Heidelberg, 2004.
Zarriess, M., Johnstone, H., Prange, M., Steph, S., Groeneveld, J., Mulitza, S., and Mackensen, A.: Bipolar seesaw in the northeastern tropical Atlantic during Heinrich stadials, Geophys. Res. Lett., 38, L04706, doi:10.1029/2010GL046070, 2011.

CPD
11, 1143–1175, 2015

Table 1. Control points used for the age model in MD03-2616, accepting the assumption of regular sediment accumulation rates between reference strata. Radiocarbon dating were carried out at the Poznan Radiocarbon Laboratory (Poz-code, Poznan, Poland) and dates were calibrated using the Marine13 curve (Reimer et al., 2013; reservoir age of 284 years and Delta R of -15 ± 37; one sigma ranges). Note that a reversal reported at cm 176 was not used in the age model, the *Pulleniatina obliquiloculata* disappearance is located at cm 288 and the LR04 benthic $\delta^{18}O_{calcite}$ stack (Lisiecki and Raymo, 2005) is used as a reference for the older sections.

Depth (cm)	Sample type	Radiocarbon Age (ka) or ref	Calibrated Age (ka BP)	Error (ka)
1	*G. sacculifer* (Poz-22 473)	5.490 ± 0.035	5.898	0.066
28	*G. sacculifer* (Poz-22 474)	10.610 ± 0.050	11.940	0.127
76	*G. sacculifer* (Poz-22 476)	12.090 ± 0.050	13.548	0.088
148	*G. sacculifer* (Poz-22 477)	22.890 ± 0.130	26.821	0.212
176	*G. sacculifer* (Poz-22 478)	19.010 ± 0.090	22.477	0.097
212	*G. sacculifer* (Poz-22 480)	26.370 ± 0.180	30.249	0.298
260	*G. sacculifer* (Poz-22 481)	30.950 ± 0.300	34.500	0.271
288	*P. obliquiloculata*	Y interval	40.000	2.000
384	*U. Peregrina*	LR04 stack	55.000	4.000
474.5	*U. Peregrina*	LR04 stack	66.300	4.000
499	*U. Peregrina*	LR04 stack	69.500	4.000
557	*U. Peregrina*	LR04 stack	73.600	4.000
701	*U. Peregrina*	LR04 stack	86.700	4.000
769	*U. Peregrina*	LR04 stack	89.500	4.000
873	*U. Peregrina*	LR04 stack	96.000	4.000
1077	*U. Peregrina*	LR04 stack	103.000	4.000
1213	*U. Peregrina*	LR04 stack	110.000	4.000
1329	*U. Peregrina*	LR04 stack	129.000	4.000

CPD
11, 1143–1175, 2015

Table 2. Trends between precession maxima and minima and vice-versa (insolation minima and maxima and vice-versa) from MIS5e to MIS2 in Greenland (NGRIP; North Greenland Ice Core Project members, 2004), Guiana (MD03-2616; this study), Cariaco (ODP 1002C; Peterson et al., 2000) and north-eastern Brazil (GeoB-3910; Jaeschke et al., 2007). *N* refers to number of samples used to calculate the trends.

MIS	Age (ka BP)	NGRIP		MD03-2616		ODP 1002		GeoB-3910	
		‰ ka^{-1}	*N*	°C ka^{-1}	*N*	% ka^{-1}	*N*	°C ka^{-1}	*N*
2	from 22.5 to 11.5	0.32	551	0.08	79	0.19	309	0.15	54
	from 33.6 to 22.5	0.01	556	−0.12	67	−0.09	248	−0.06	43
3	from 46.8 to 33.6	−0.13	661	0.01	42	0.07	355	0.03	72
	from 60.1 to 46.8	−0.04	666	0.05	53	0.43	300	0.02	47
4	from 71.6 to 60.1	−0.16	576	−0.16	63	−0.26	192		
5a	from 82.7 to 71.6	−0.38	556	−0.07	38	−0.14	117		
5b	from 94.2 to 82.7	0.08	576	−0.04	52				
5c	from 105.4 to 94.2	−0.11	561	−0.01	82				
5d	from 116.3 to 105.5	−0.08	541	−0.03	47				
5e	from 127.3 to 116.3	−1.27	300	−0.05	21				

CPD
11, 1143–1175, 2015

Table 3. Changes defined as positive or negative increments represented by ≥ 3 samples, occurring faster than the average SST warming during the last deglaciation, $+2\,^{\circ}\mathrm{C\,ka^{-1}}$ ($3.1\,^{\circ}\mathrm{C}$ in 1550 years in the MD03-2616 record) and higher than $\pm 0.5\,^{\circ}\mathrm{C}$.

MIS	Events	Onset cm	End cm	Onset ka	End ka	Onset °C	End °C	Δ °C	Δ ka	°C ka^{-1}
2	1	28	21	11.770	10.247	25.1	28.2	3.1	1.5	2.0
	2	51	45	12.707	12.507	25.9	27.4	1.4	0.2	7.2
3	3	210	206	30.133	29.918	26.3	27.3	1.0	0.2	4.7
	4	214	211	30.422	30.186	26.2	27.4	1.2	0.2	5.1
	5	400	395	57.002	56.377	25.9	27.2	1.4	0.6	2.2
5	6	701	693	87.565	87.194	26.7	27.6	0.9	0.4	2.4
	7	685	677	86.865	86.700	27.3	27.9	0.6	0.2	3.5
	8	1129	1121	105.676	105.265	27.3	28.2	0.8	0.4	2.0
2	1	45	34	12.507	12.140	27.4	25.2	−2.2	0.4	−5.9
	2	55	51	12.840	12.707	26.9	25.9	−1.0	0.1	−7.4
	3	62	56	13.073	12.873	27.2	26.0	−1.3	0.2	−6.3
	4	77	72	13.724	13.407	27.5	26.0	−1.5	0.3	−4.8
4	5	182	176	28.628	28.305	27.1	26.0	−1.1	0.3	−3.3
	6	222	216	31.148	30.603	27.4	26.2	−1.2	0.5	−2.1
	7	505	499	69.939	69.517	28.1	26.6	−1.5	0.4	−3.5

CPD
11, 1143–1175, 2015

Parallelisms between sea surface temperature changes in the western tropical Atlantic

O. Rama-Corredor et al.

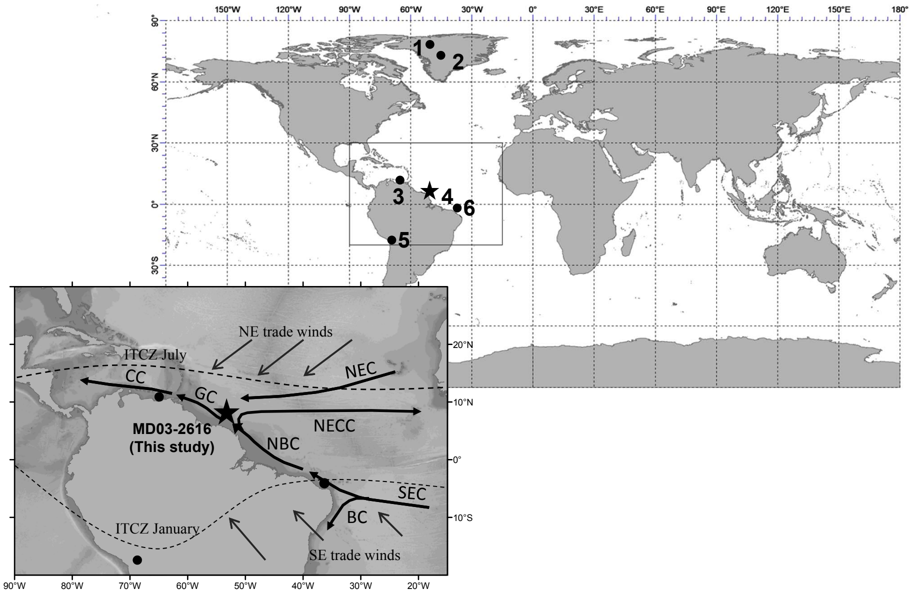

Figure 1. Map showing the sites mentioned in the text: 1 – NEEM (NEEM community members, 2013), 2 – NGRIP (Wolff et al., 2010), 3 – ODP 1002 (Peterson et al., 2000), 4 – MD03-2616, this study (7.4875° N, 53.0080° W, −1233 m below sea level), 5 – Sajama ice-core (Thompson et al., 1998). 6 – GeoB-3910 (Jaeschke et al., 2007). Guiana current (GC), ITCZ and trade winds are shown (north-easterlies when the ITCZ moves north of the Equator and south-easterlies when it moves southward).

CPD
11, 1143–1175, 2015

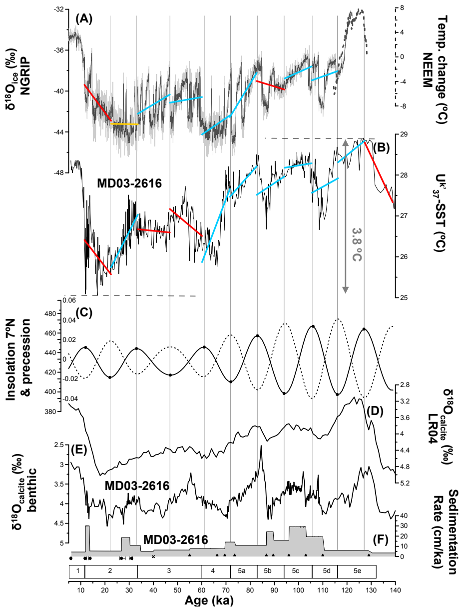

Figure 2. Guiana SSTs versus Greenland and orbital changes. **(a)** $\delta^{18}O_{ice}$ (‰) NGRIP (GICC05 modelext time scale) (Wolff et al., 2010; Svensson et al., 2011) and temperature change in NEEM (dashed line; NEEM community members, 2013), **(b)** MD03-2616 $U^{\prime k}_{37}$-SST (this study). **(c)** Precessional changes, which are inversely related to the daily insolation at 7° N during the summer solstice (Berger, 1978). **(d)** LR04 stack (Lisiecki and Raymo, 2005). **(e)** MD03-2616 $\delta^{18}O_{calcite}$ benthic, **(f)** MD03-2616 Sedimentation rate over time at core location (this study). Control points used for the age model (Table 1) are shown: dots for AMS-^{14}C dates; a cross for the *Y* bioclimatic event and triangles for tie-points between MD03-2616 benthic isotopes (López-Otálvaro et al., 2009) and the LR04 stack (Lisiecki and Raymo, 2005). Trends between perihelion passage in the NH summer (precession minima; insolation maxima) and winter solstices (precession maxima; insolation minima) are shown for NGRIP and MD03-2616; warming trends in red and cooling trends in blue.

CPD

11, 1143–1175, 2015

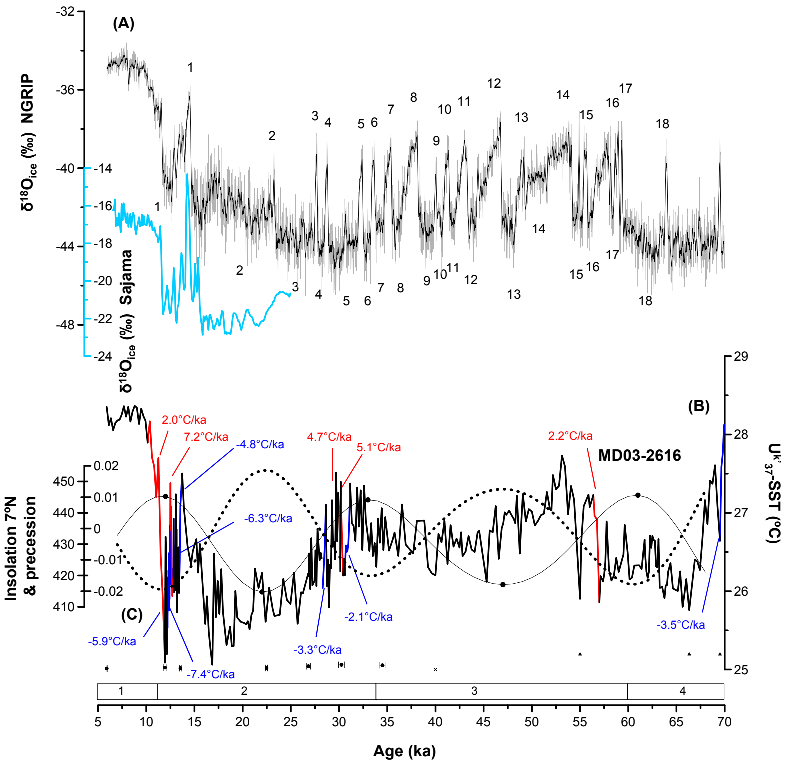

Figure 3. Abrupt changes over MIS4, MIS3 and MIS2. **(a)** $\delta^{18}O_{ice}$ (‰) measured in NGRIP (North Greenland Ice Core Project members, 2004; Wolff et al., 2010) and in the Sajama ice core (Thompson et al., 1998). **(b)** MD03-2616 $U^{\prime k}_{37}$-SST (this study). **(c)** Precession and daily insolation at 7° N during the summer solstice (Berger, 1978). Abrupt changes identified in the MD03-2616 SST record are operationally defined as a transition faster than 2 °C ka^{-1} and with absolute intensity equal or higher than 0.5 °C (Table 3). Changes plotted as blue (cooling) or red (warming) lines.

CPD
11, 1143–1175, 2015

Parallelisms between sea surface temperature changes in the western tropical Atlantic

O. Rama-Corredor et al.

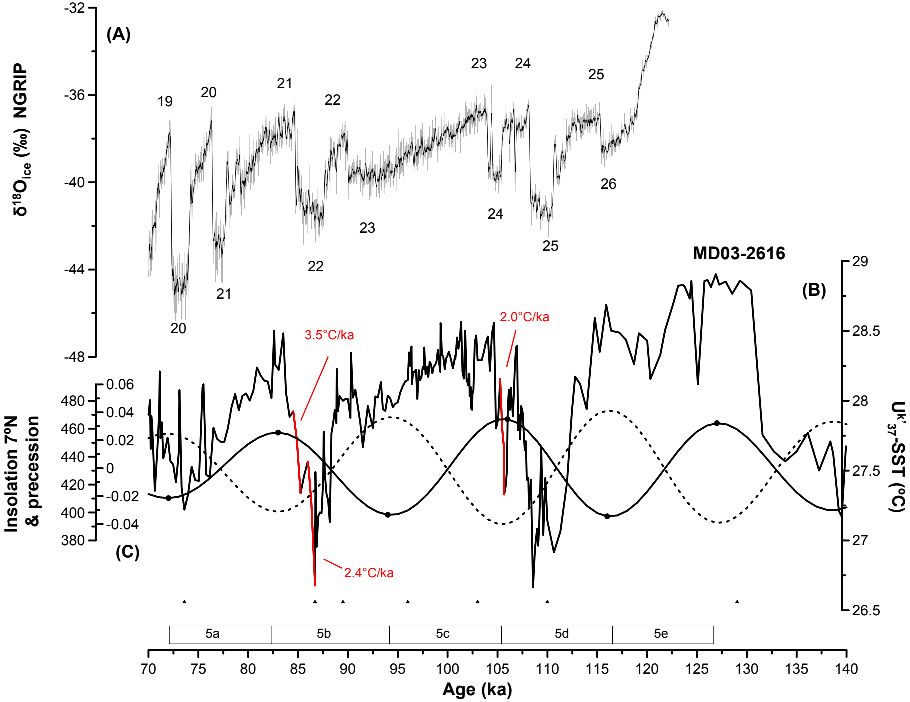

Figure 4. Abrupt changes over MIS5e-a. **(a)** $\delta^{18}O_{ice}$ (‰) measured in NGRIP (North Greenland Ice Core Project members, 2004; Wolff et al., 2010). **(b)** MD03-2616 $U^{\prime k}_{37}$-SST (this study). **(c)** Precession and daily insolation at 7° N during the summer solstice (Berger, 1978). Abrupt temperature changes (higher than 0.5 °C and 2 °C ka^{-1}) are plotted as blue (cooling) or red (warming) lines.

CPD
11, 1143–1175, 2015

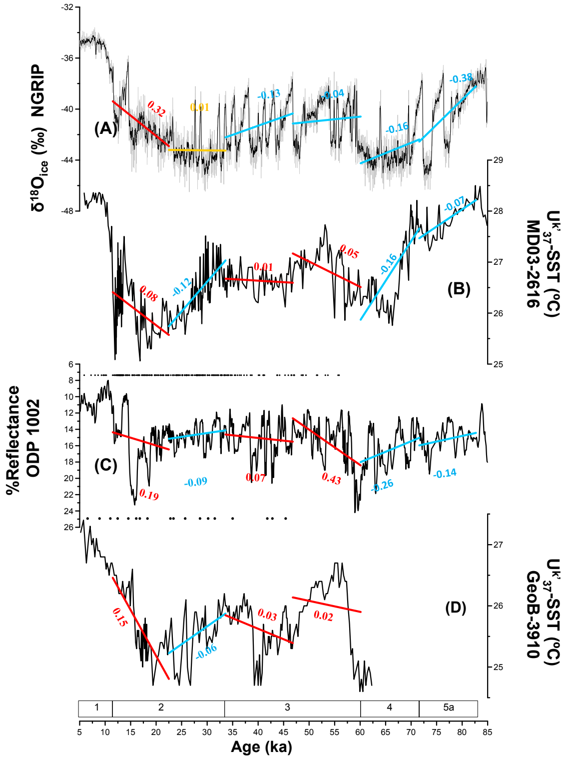

Figure 5. Glacial see-saw between Greenland and Guiana. **(a)** $\delta^{18}O_{ice}$ measured in NGRIP (North Greenland Ice Core Project members, 2004; Wolff et al., 2010). **(b)** MD03-2616 $U_{37}^{\prime k}$-SST (this study). **(d)** %Reflectance in ODP 1002, Cariaco (Peterson et al., 2000). **(e)** GeoB-3910 $U_{37}^{\prime k}$-SST, north-eastern Brazil (Jaeschke et al., 2007). Trends between precession maxima and minima and vice-versa are shown and numbers close to trends refer to values in Table 2. Radiocarbon dates are drawn as dots on the top of the ODP 1002 and GeoB-3910 profiles.

CPD
11, 1143–1175, 2015

Parallelisms between sea surface temperature changes in the western tropical Atlantic

O. Rama-Corredor et al.